Wave-Beam Shaping Using Multiple Phase-Correction Mirrors

Yosuke Hirata, Yoshika Mitsunaka, Kenichi Hayashi, and Yasuyuki Itoh

***Abstract*— This paper describes a scheme for shaping a given wave beam into the desired profile using multiple phase-correction mirrors. This mirror system was applied to a gyrotron internal converter to flatten the radiated beam profile at the window. The flat output beam is reconverted into HE11 mode, a basic propagation mode for corrugated waveguides, by another pair of phase-correction mirrors for transmission into a fusion reactor. In addition, a wave-beam splitting and combining technique is also presented.**

***Index Terms*— Gyrotron, phase-correction mirror, shaping, wave-beam window.**

I. Introduction

CURRENT problems in gyrotron research include window failure due to dielectric loss from the transmitted wave beam. In the case of a conventional face-cooled window with a Gaussian beam output, high-power transmissions can induce boiling of the coolant and window damage. If the gyrotron output could be extracted in a wave beam with a flat power profile, it would be possible to reduce the peak power density of the output wave, thereby suppressing coolant boiling. Fig. 1 is a schematic drawing of a typical gyrotron converter and mirror system. A Vlasov-type mode converter [1] or a dimple mode converter [2] is incorporated in the gyrotron to transform the cavity-excited circular-waveguide mode into a wave beam. The wave beam travels through the mirror system, which converts it into a Gaussian-like beam, to the output window. Several efforts have been made to broaden the output wave-beam profile using internal mirrors [3]–[5]. These attempts focused only on shaping the power profile of the mode converter output.

On the other hand, where the gyrotron output is conveyed to a fusion device at a typical distance of about 100 m, corrugated waveguides are used. To minimize losses, the gyrotron output is ideally converted into the HE11 mode, which propagates in corrugated waveguides with very low transmission loss. Coupling efficiency with the corrugated waveguide strongly depends on both the power and phase profiles of the converted wave beam. However, there has been no attempt to transform the power and phase of a given wave beam into the desirable profiles.

Itoh (one of the authors of this paper) and Sugawara proposed a scheme for designing shaping mirrors, in the axisymmetric system, that are able to transform any wave beam into one with the desired power and phase profiles [6].

Manuscript received March 5, 1996; revised September 23, 1996.

The authors are with the Energy and Mechanical Research Laboratories, Toshiba Corporation, Kawasaki 210, Japan.

Publisher Item Identifier S 0018-9480(97)00267-6.

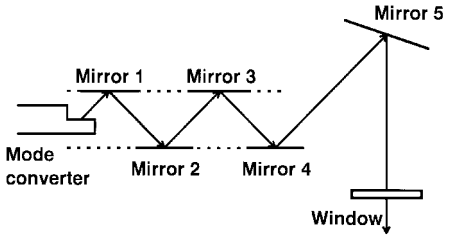

Fig. 1. Gyrotron internal mirror system.

In this work, we studied shaping-mirror design in the two-dimensional system and applied the newly designed mirrors to an internal converter for a gyrotron in order to flatten the power and phase profiles of the output wave at the window.

As another application of this shaping-mirror design, we offer wave-beam splitting and recombining mirrors applicable to multimegawatt gyrotrons. Since the double disk window system is unable to withstand the transmission of multi-megawatt, continuous wave beams at around 170 GHz, it has been suggested that the cavity output may be split into multiple beams by means of an internal mode converter or an internal mirror system. The multiple wave beams are then extracted through multiple windows [7], [8]. However, no studies for recombining the multiple outputs into one beam have been carried out, and extracting the gyrotron output through multiple windows, which requires multiple transmission lines for each gyrotron, will increase the construction cost of transmission lines. In this paper, we design a set of shaping mirrors that split the cavity output into multiple wave beams and another set of mirrors to recombine them into a single beam for transmission.

In Section II of the paper, we consider a design scheme for the shaping mirrors. Section III offers examples of the above shaping-mirror applications. Conclusions are given in Section IV.

II. Design Scheme

We consider the transformation of the power and phase profiles of an input wave by means of two phase-correction mirrors, as shown in Fig. 2. In the design process, the mirrors are treated as lenses. The lens model gives a good approximation for paraxial waves whose local wave vectors are almost in the same direction as the whole-wave propagation [5], [6].

If the wave function is $u(\boldsymbol{r})e^{-j\omega t}$, the surface deformation of a mirror, $h(\boldsymbol{r})$, causes the approximate local phase deformation

$$\Delta\phi(\boldsymbol{r}) = -2kh(\boldsymbol{r})\cos\alpha \tag{1}$$

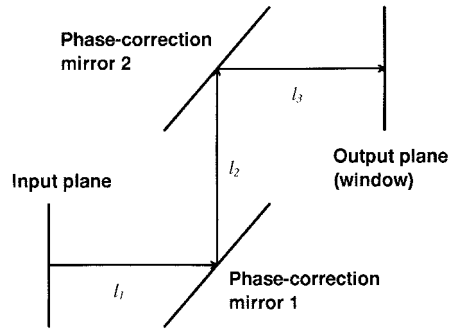

Fig. 2. Mirror system comprising two phase-correction mirrors.

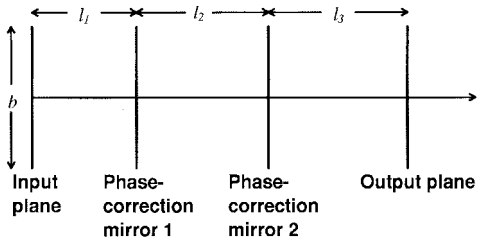

Fig. 3. Equivalent wave path in lens approximation.

between the incident and reflected waves, where k is the wave number and α is the wave incident angle. If we assume the input wave function to be $u^i(\boldsymbol{r})$ and the reflected wave to be $u^r(\boldsymbol{r})$, the two functions are related by the equation:

$$u^r(\boldsymbol{r}) = u^i(\boldsymbol{r})e^{j\phi(r)}. \tag{2}$$

An equivalent wave path using the lens approximation is illustrated in Fig. 3.

If perfect transformation of the power and phase profiles of an input wave is achieved, a wave beam with the same power and phase profiles as the input wave should be obtained if the desired wave is transmitted backward from the output plane. To seek this ideal transformation, we focus on the phase of the forward and backward waves at the two mirror surfaces. A wave beam with the desired power and phase profiles is transmitted backward from the output plane. The surface deformation functions of the two shaping mirrors, $h_1(\boldsymbol{r})$ and $h_2(\boldsymbol{r})$, are determined self-consistently in such a way that the phase of the forward wave, $\phi_f(\boldsymbol{r}_M)$, and the phase of the backward wave, $\phi_b(\boldsymbol{r}_M)$, satisfy the condition $\phi_f(\boldsymbol{r}_M) + \phi_b(\boldsymbol{r}_M) = \text{const.}$ at all points on both the first and second mirror surfaces. Here, $\boldsymbol{r}_M$ denotes a point on the phase-correction mirror surface.

With the lens approximation, the design calculation is performed in the following manner [6]. We write the input wave function on the input plane and the desired wave function on the output plane as $u_i(x, y, z = 0)$ and $u_o(x, y, z = z_o)$, respectively. These waves propagate in the $+z$ direction. The backward wave with the desired profile on the output plane can be written as $u_o^*(x, y, z)$. First, we assume $h_1(x, y) = h_1^0(x, y)$ with $h_1^0(x, y)$ being a guessed function. Using this surface function combined with (1) and (2), the wave function of the input wave at the second mirror position, $z = z_2$, is calculated. Then, the backward wave function at the second mirror, $u_o^*(x, y, z_2)$, is calculated. The second mirror surface, $h_2^1(x, y)$, is determined in such a way that the phase of both the forward wave, $\mathrm{Arg}[u_i(x, y, z_2)]$, and the complex conjugate of the phase of the backward wave, $\mathrm{Arg}[u_o(x, y, z_2)]$, satisfy

$$\begin{aligned} -2kh_2^1(x, y)\cos\alpha &= \mathrm{Arg}[u_o(x, y, z_2)] - \mathrm{Arg}[u_i(x, y, z_2)] \\ &= \Delta\phi(x, y). \end{aligned} \tag{3}$$

Next, using the second mirror surface just obtained, $h_2^1(x, y)$, the backward wave function is calculated at the first mirror position. The surface function of the first mirror, $h_1^1(x, y)$, is determined in such a way that the phase of both the forward and backward waves satisfies (3) at all points on the first mirror surface. Then, the second mirror function, $h_2^2(x, y)$, is again determined using $h_1^1(x, y)$, and so on. This iterative calculation is completed when the mirror functions or the wave-beam profiles converge.

In the determination of the mirror surface functions, the wave-beam propagation is analyzed using the plane-wave expansion [9] for calculation with the fast Fourier transformation (FFT) [10]. The wave profile on the input plane is given by

$$\begin{aligned} u_i(x, y) &= u(x, y, 0) \\ &= \frac{1}{4\pi^2}\int_{-\infty}^{\infty}\int_{-\infty}^{\infty}\tilde{u}(k_x, k_y)e^{j(k_x x + k_y y)}\,dk_x\,dk_y \end{aligned}$$

where

$$\tilde{u}(k_x, k_y) = \int_{-\infty}^{\infty}\int_{-\infty}^{\infty}u(x, y, 0)e^{-j(k_x x + k_y y)}\,dx\,dy.$$

The wave profile at $z = z_l$ is then

$$\begin{aligned} &u(x, y, z_l) \\ &\quad = \frac{1}{4\pi^2}\int_{-\infty}^{\infty}\int_{-\infty}^{\infty}\tilde{u}(k_x, k_y)e^{j(k_x x + k_y y + k_z z_l)}\,dk_x\,dk_y \end{aligned}$$

where

$$k_z = \sqrt{k^2 - k_x^2 - k_y^2}.$$

Modes with pure imaginary k_z are evanescent and are not considered.

The required computational time in a single iteration for 128 × 128 complex data is 1.8 s using an IBM RS/6000 model 3BT. The typical iteration number during calculations is 50–100.

III. Shaping-Mirror Applications

A. Wave-Beam Flattening

This section gives examples of shaping-mirror applications. First, we consider transforming the output of a mode converter into a wave beam with flat power and phase profiles. Here, we adopted a dimple mode converter, which converts the cavity-generated wave into a wave beam at an efficiency of over 95% [2]. Fig. 4 illustrates the power profile of a dimple mode

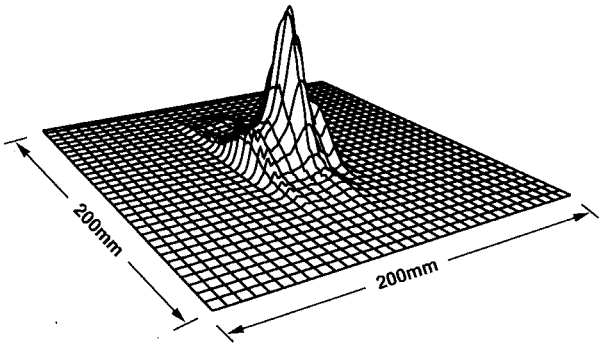

Fig. 4. Power profile of a dimple mode converter output.

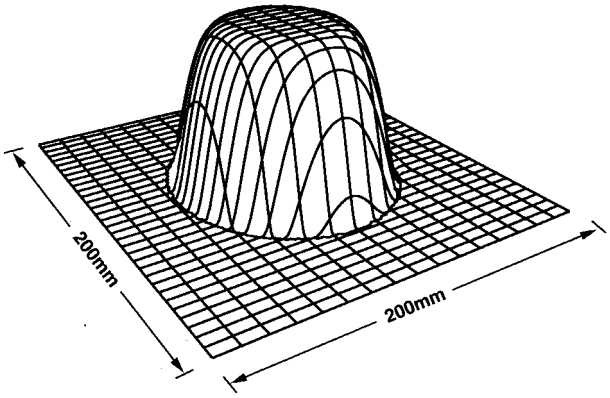

Fig. 5. Target power profile on the output plane.

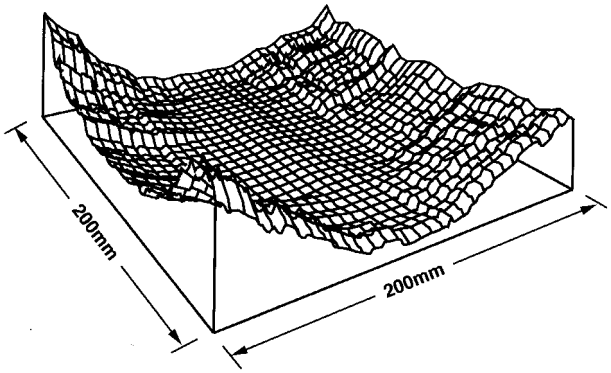

Fig. 6. Resulting surface of the first mirror.

converter output on the input plane. The target wave has a uniform phase distribution; its power profile is given by

$$P(r) \propto \{1 - (r/a)^8\}^2 \quad \text{with } a = 0.06 \text{ m}$$

which is determined in consideration of a typical window size of ϕ140 mm. Fig. 5 illustrates the power profile of the target wave on the output plane. The mirrors were designed using the equivalent wave path shown in Fig. 3 with $l_1 = 0.2$ m and $l_2 = l_3 = 0.5$ m. The size of these mirrors was $0.2 \text{ m} \times 0.2$ m. The iterative calculation was completed when the target and calculated power profiles on the output plane converged.

Surface functions of the two shaping mirrors were determined in the manner described in Section II. The resulting surfaces of the two mirrors are illustrated in Figs. 6 and 7. The maximum mirror height was about 5 mm. Fig. 8 shows

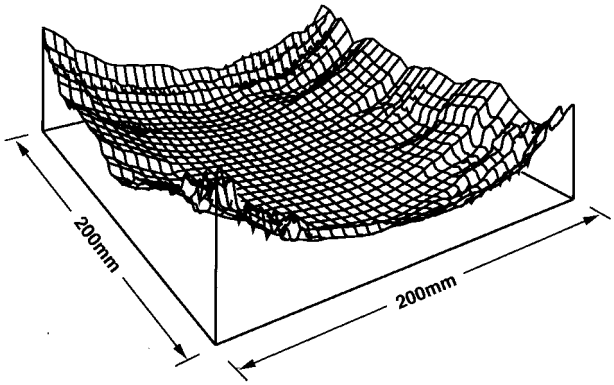

Fig. 7. Resulting surface of the second mirror.

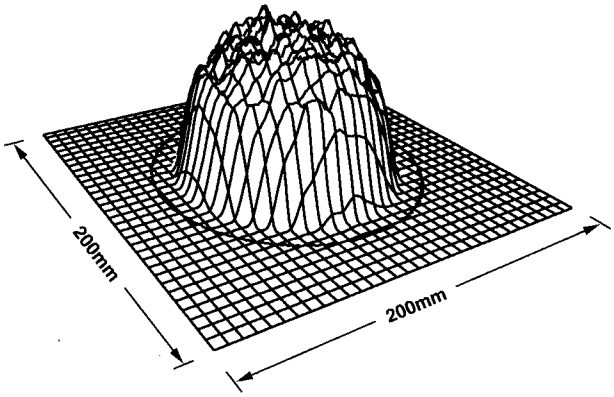

Fig. 8. Achieved power profile on the output plane.

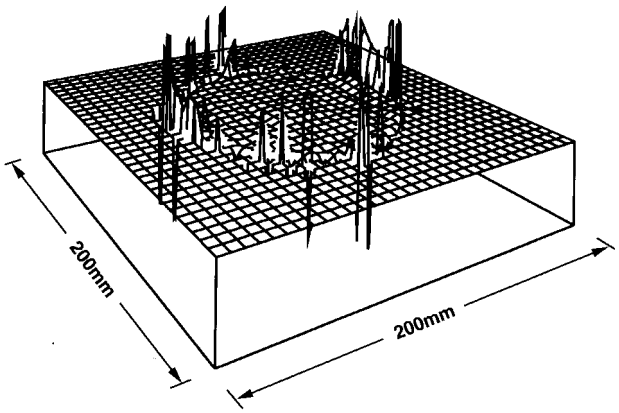

Fig. 9. Achieved phase profile on the output plane.

the achieved power profile on the output plane; Fig. 9 gives its phase profile. The wave profiles of Figs. 5 and 8 are in good agreement, demonstrating the propriety of this shaping-mirror design. Fig. 9 shows that the phase of the obtained wave is also flat on the output plane. The FFT-calculated propagation efficiency through the mirror system was over 99%.

In the second part of this example, the obtained flat gyrotron output is reconverted into the HE11 mode for transmission through 88.9-mm-diameter corrugated waveguides. The calculation was carried out for the mirror system illustrated in Fig. 3 with $l_1 = 1.0$ m and $l_2 = l_3 = 0.5$ m. Once again the mirror size was $0.2 \text{ m} \times 0.2$ m. Here, we consider the gyrotron

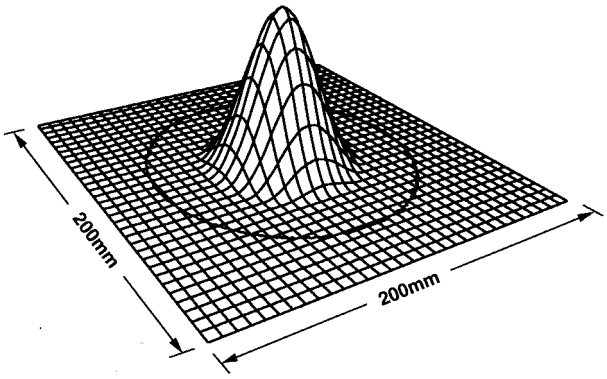

Fig. 10. Achieved power profile at the corrugated waveguide entrance.

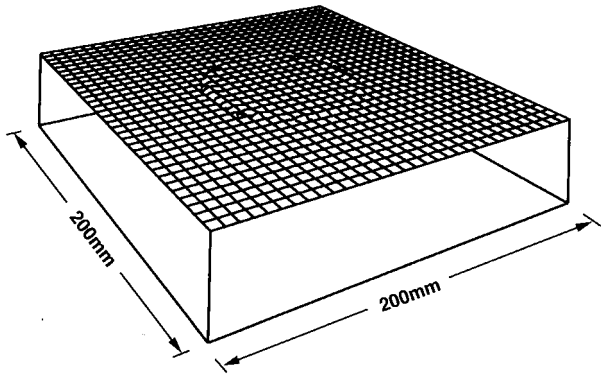

Fig. 11. Achieved phase profile at the corrugated waveguide entrance.

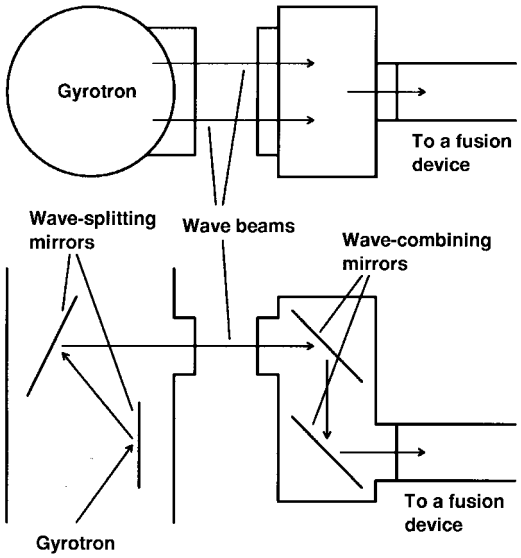

Fig. 12. Concept of wave splitting and combining.

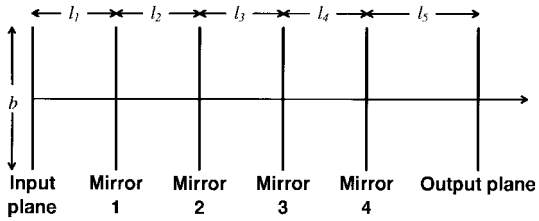

Fig. 13. Equivalent wave path in lens approximation.

window as the input plane and the entrance to the corrugated waveguide as the output plane. Fig. 10 depicts the wave-power profile obtained on the output plane. Fig. 11 illustrates its phase distribution. Both power and phase profiles are in good agreement with the target HE11 mode. More than 99% of the power passing through the input plane is transmitted into the corrugated waveguide. The HE11 component of the obtained beam is 99.6%, demonstrating the high coupling efficiency with the corrugated waveguide.

B. Wave-Beam Splitting and Combining

Our second example involves transforming the dimple mode converter output into two flat beams for use with multimegawatt gyrotrons. The wave-beam splitting and combining concept is illustrated in Fig. 12. Here, four phase-correction mirrors are employed to improve conversion efficiency. Fig. 13 illustrates the equivalent wave path where $l_1 = l_2 = l_3 = l_4 = 0.1$ (m) and $l_5 = 0.5$ (m). The assumed mirror size was 0.3 (m) $\times$ 0.3 (m).

The four shaping mirrors were designed in the following manner. 1) The first and fourth mirrors were designed under the assumption that the second and third mirrors are both flat. 2) Then, for the input wave phase-corrected by the first mirror and the output wave phase-corrected by the fourth mirror, the remaining second and third mirrors were determined. Thus, the four resulting mirrors transform the converter output into two flat beams with a diameter of 0.11 m. Fig. 14 shows the power distribution of the obtained wave on the output plane. Fig. 15 gives its phase profile. The converter output was well split into two flat beams.

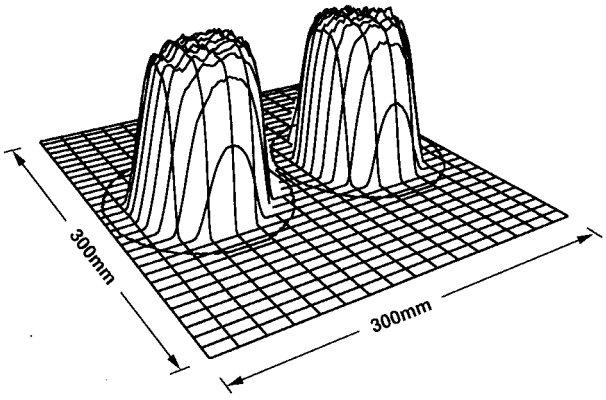

Fig. 14. Achieved power profile at the window position.

These two flat beams are reconverted into the HE11 mode, for transmission, using four phase-correction mirrors. The mirror separations are $l_1 = l_2 = l_3 = l_4 = l_5 = 0.1$ m. Fig. 16 illustrates the power distribution on the output plane, namely, the entrance to the corrugated waveguide. Fig. 17 depicts its phase distribution. The calculated transmission efficiency from the input plane of the wave-splitting mirror system to the entrance of the corrugated waveguide is 99% with an HE11 component of 99.8%.

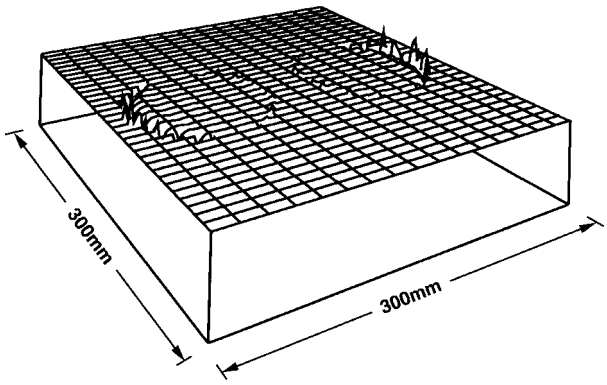

Fig. 15. Achieved phase profile at the window position.

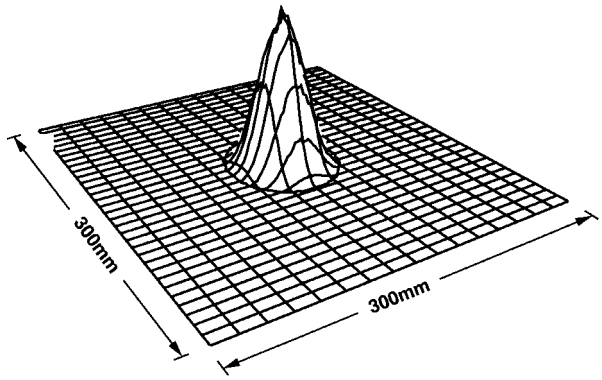

Fig. 16. Achieved power profile at the corrugated waveguide entrance.

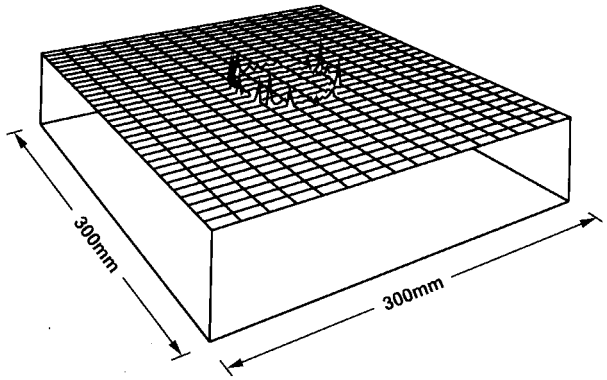

Fig. 17. Achieved phase profile at the corrugated waveguide entrance.

IV. Conclusions

We have studied a method for transforming both the power and phase of a given wave beam into desired profiles using multiple phase-correction mirrors. Using this method with an FFT-based wave propagation code, two shaping mirrors were designed that transform the output of a dimple mode converter into a wave beam with flat power and phase profiles at the gyrotron window position. Good agreement was achieved between the desired and obtained profiles. The resulting flat gyrotron output was retransformed into the HE11 mode for transmission to a fusion reactor. The HE11 component of the obtained wave at the corrugated waveguide entrance was 99.6% with a transmission efficiency of 99%.

Mirrors that transform a converter output into two flat beams were also designed with a view to application in multimegawatt gyrotrons. Four phase-correction mirrors were used to improve conversion efficiency. The converter output was well split into two flat beams. These flat beams were reconverted into the HE11 mode. The calculated HE11 component was 99.8% with a transmission efficiency of 99%.

References

[1] S. N. Vlasov, L. I. Sagryadskaya, and M. I. Petelin, "Transformation of a whispering gallery mode, propagating in a circular waveguide, into a beam of waves," *Radio Eng. Electron. Phys.*, vol. 21, no. 10, pp. 14–17, 1975.

[2] G. G. Denisov, A. N. Kuftin, V. I. Malygin, Np. P. Venediktov, D. V. Vinogradov, and V. E. Zapevalov, "110 GHz gyrotron with a built-in high-efficiency converter," *Int. J. Electron.*, pp. 1079–1091, 1992.

[3] M. V. Agapove, L. A. Axenov, V. V. Alikaev, A. P. Cayer, G. G. Denisov, V. A. Fljagin, A. Sh. Fix, V. I. Iljin, V. N. Ilyin, V. A. Khmara, A. N. Kostyna, A. N. Kuftin, V. E. Mjasnikov, L. G. Popov, and V. E. Zapevalov, "Long-pulsed 140-GHz/0.5-MW gyrotron: Problems and results," in *Conf. Dig. 19th Int. Conf. Infrared Millimeter Waves*, 1994, pp 79–80.

[4] K. Felch, T. S. Chu, W. DeHope, H. Huey, H. Jory, J. Neilson, and R. Schumacher, "Recent test results on a high-power gyrotron with an internal, quasi-optical converter," in *Conf. Dig. 19th Int. Conf. Infrared Millimeter Waves*, 1994, pp. 333–334.

[5] A. A. Bogdashov, A. V. Chirkov, G. G. Denisov, D. V. Vinogradov, A. N. Kuftin, V. I. Malygin, and V. E. Zapevalov, "Mirror synthesis for gyrotron quasi-optical mode converters," *Int. J. Infrared Millimeter Waves*, vol. 16, no. 4, pp. 735–744, 1995.

[6] Y. Itoh and T. Sugawara, *Int. J. Infrared Millimeter Waves*, vol. 17, no. 2, pp. 465–475, 1996.

[7] Y. Hirata, Y. Mitsunaka, K. Hayashi, Y. Itoh, and T. Sugawara, "Design of a 1-MW, CW, coaxial gyrotron with two Gaussian beam outputs," *Int. J. Infrared Millimeter Waves*, vol. 16, no. 4, pp. 713–733, 1995.

[8] M. Blank, K. E. Kreischer, and R. J. Temkin, "Experimental study of a quasi-optical mode converter for a 110 GHz gyrotron," in *Conf. Dig. 19th Int. Conf. Infrared Millimeter Waves*, 1994, pp. 331–332.

[9] K. Ohkubo, M. Hosokawa, S. Kubo, M. Sato, Y, Takita, and T. Kuroda, "R&D of transmission lines for ECH System," NIFS Rep. 210, National Institute of Fusion Science, 1993.

[10] W. H. Press, B. P. Flannery, S. A. Teukolsky, and W. T. Vetterling, *Numerical Recipes in C.* Cambridge, U.K.: Cambridge Univ. Press, 1988, p. 407.

Yosuke Hirata was born in Osaka, Japan, on March 5, 1965. He received the B.S. and M.S. degrees in nuclear engineering from Kyoto University, Kyoto, Japan, in 1987 and 1989, respectively.

He joined the Research and Development Center of Toshiba Corporation in 1989 where he has been engaged in the study of high-power gyrotrons and high-power millimeter-wave transmission.

Yoshika Mitsunaka was born in Mie, Japan, on November 3, 1961. He received the B.S. and M.S. degrees in nuclear engineering from Nagoya University, Nagoya, Japan, in 1984 and 1986, respectively.

He has been working at the Research and Development Center of Toshiba Corporation where he is engaged in gyrotron development. His interests are in numerical simulation and experimental investigation of mode converters and quasi-optical transmission lines inside and outside of gyrotron tubes.

Kenichi Hayashi was born in Yamaguchi, Japan, on February 3, 1955. He received the B.S. and M.S. degrees from Osaka University, Osaka, Japan, in 1977 and 1979, respectively.

Since 1979, he has been with the Research and Development Center of Toshiba Corporation. His research interests are in high-power millimeter-wave sources.

Yasuyuki Itoh was born in Hiroshima, Japan, on January 24, 1953. He received the B.S., M.S., and Ph.D. degrees in nuclear engineering from Osaka University, Osaka, Japan in 1975, 1977, and 1981, respectively.

In 1981 he joined the Research and Development Center of Toshiba Corporation. His research interests include quasi-optical technique and high-power millimeter-wave transmission lines.

A Millimeter-Wave Band MMIC Dual-Quadrature Up-Converter Using Multilayer Directional Couplers

Akira Minakawa, *Member, IEEE,* Toshikazu Imaoka, *Member, IEEE,* and Nobuaki Imai, *Member, IEEE*

***Abstract*—This paper describes a newly developed monolithic-microwave integrated circuit (MMIC) dual-quadrature up-converter with very high local oscillator (LO) signal leakage suppression and good LO and RF return loss for use in the millimeter-wave band. The dual-quadrature LO suppression technique is also described, and the requirements for an imbalance in the quadrature couplers to obtain large LO suppression are clarified. The up-converter consists of two unit mixers and two high-performance multilayer directional couplers. These high-performance directional couplers enable large LO suppression. In an LO frequency range from 42.5 to 47.5 GHz, the MMIC up-converter achieved a conversion loss of less than 17±1 dB, and the LO was suppressed 22±4 dB lower than the desired RF output signal, which is the greatest value among those reported.**

I. Introduction

THE SMALL size and reproducible performance of monolithic-microwave integrated circuits (MMIC's) are contributing greatly to reductions in the cost and size of microwave/millimeter-wave circuits. A frequency up-converter is one of the most important circuits in microwave/millimeter-wave radio systems. In an up-converter, it is difficult to reject a local oscillator (LO) signal using a filter because the LO and desired radio-frequency (RF) signals are close in frequency. In order to provide good LO signal leakage suppression without using filters at the RF output port, up-converters often employ a balanced-type configuration. In addition, since filters are difficult to implement on an MMIC chip due to the MMIC's low Q property, a balanced-type configuration is extremely practical in MMIC's.

A few reports about millimeter-wave band MMIC up-converters have been published [1], [2]. Hirota *et al.* [1] have reported an MMIC balanced up-converter with a 50–62-GHz operating frequency range. This up-converter has a very small chip size, but maximum LO leakage suppression is 12 dB. Wang *et al*. [2] have reported a diode-balanced up-converter with a 56–64-GHz operating frequency range, but they do not mention LO leakage suppression.

In this paper, we describe a newly developed millimeter-wave band MMIC dual-quadrature up-converter with a balanced-type configuration. A dual-quadrature type has the advantage of good LO and RF return loss characteristics. The up-converter employs new multilayer directional couplers [3], which were developed in our laboratories as high-performance 3-dB quadrature divider/combiner circuits. A multilayer MMIC technique [4], [5] is also employed to improve the design flexibility. The requirements for an imbalance in the quadrature couplers to obtain large LO suppression are clarified. Based on this design, an LO leakage suppression of 22±4 dB lower than the desired RF output signal could be achieved, and good LO and RF return loss in the millimeter-wave band could also be achieved.

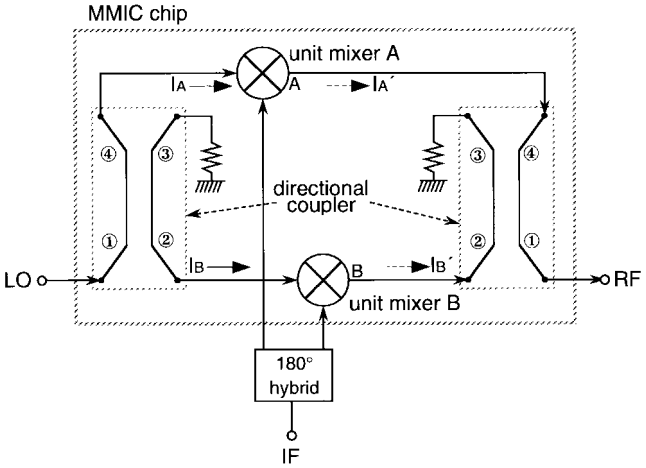

Fig. 1. Block diagram of the MMIC dual-quadrature up-converter.

II. MMIC Dual-Quadrature Up-Converter Design

A. Circuit Configuration

A block diagram of the MMIC dual-quadrature up-converter is shown in Fig. 1. It consists of two identical unit mixers, which are single-ended up-converters, and two newly developed multilayer directional couplers, which are 3-dB quadrature divider/combiner circuits. The IF input signal is split into out-of-phase signals using a 180° hybrid that is externally connected. The dual usage of the 3-dB quadrature coupler provides two important characteristics: good LO to RF isolation without filters and good LO and RF return loss.

Here we explain how the 3-dB quadrature coupler provides good LO return loss. This approach is similar to that used with balanced amplifiers using 3-dB quadrature couplers. Since the two unit mixers are identical, reflection coefficients of the unit mixers are equal and reflected signals from unit

Manuscript received March 15, 1996; revised September 23, 1996.

A. Minakawa was with ATR Optical and Radio Communications Research Laboratories, Kyoto 619-02, Japan. He is now with NTT Wireless Systems Laboratories, Yokosuka-shi 239, Japan.

T. Imaoka and N. Imai were with ATR Optical and Radio Communications Research Laboratories, Kyoto 619-02, Japan. They are now with ATR Adaptive Communications Research Laboratories, Kyoto 619-02, Japan.

Publisher Item Identifier S 0018-9480(97)00268-8.

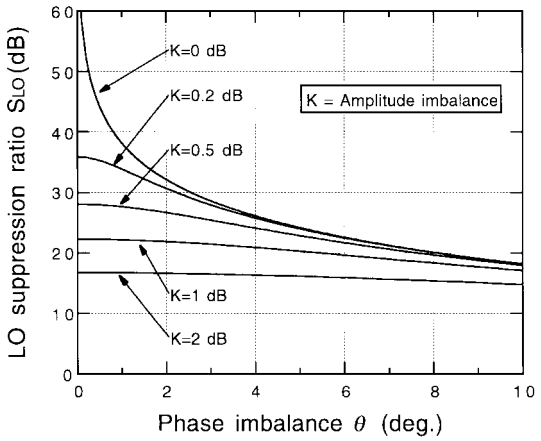

Fig. 2. LO suppression ratio versus phase and amplitude imbalance.

mixers A and B retain their quadrature and equal amplitude relationship. Because the reflected signal from unit mixer A is shifted an additional 90°, the two reflected signals from unit mixers A and B are canceled at the LO input port and the dual-quadrature up-converter has a good LO input return loss. Likewise, the dual-quadrature up-converter has good RF return loss.

B. Up-Converting Process

As shown in Fig. 1, the LO signal is fed to the unit mixer through an LO directional coupler, and the IF signal is fed through an external 180° hybrid. This provides a 90° phase difference between the LO and IF signals applied to the unit mixers. The two up-converted RF signals and the two LO leakage signals $I'_{\rm A}$ and $I'_{\rm B}$ appear at the outputs of the mixers. The RF signal at point B is $+90°$ relative to point A, and the LO leakage signal $I'_{\rm B}$ at point B is $-90°$ relative to point A. These signals are combined in an RF directional coupler. As a result, the LO leakage signals are canceled, and only the RF output signal remains.

C. LO Leakage Suppression

As mentioned above, under ideal conditions (perfect quadrature couplers and identical unit up-converters), LO leakage signals are completely canceled. However, the LO leakage signals are not completely canceled because the quadrature couplers and unit mixers used in a practical up-converter have both phase and amplitude imbalance. In this section, we will give the relationship between LO leakage suppression and amplitude/phase imbalance.

Unit mixers A and B have LO leakage currents $I'_{\rm A}$ and $I'_{\rm B}$ respectively (see Fig. 1). $I'_{\rm A}$ and $I'_{\rm B}$ are combined at the RF quadrature coupler. If the phase difference of the quadrature couplers deviates from 90°, or if the output current $I'_{\rm A}$ is not equal to $I'_{\rm B}$, LO leakage current $I_{\rm leak}$ appears at the RF output port. $I_{\rm leak}$ is expressed as

$$I_{\rm leak} = \sqrt{I'^2_{\rm A} + I'^2_{\rm B} - 2 \cdot I'_{\rm A} \cdot I'_{\rm B} \cdot \cos\theta} \tag{1}$$

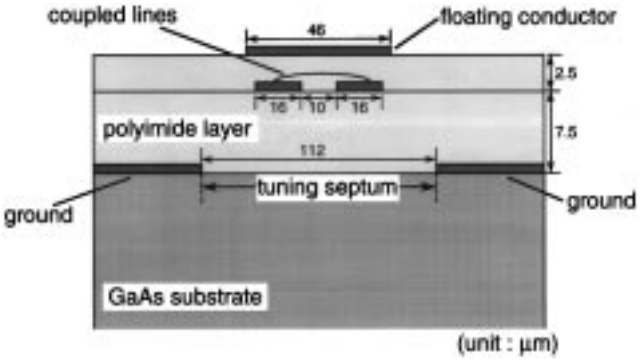

Fig. 3. Cross-sectional view of the multilayer directional coupler used for the up-converter.

where θ is the total phase imbalance. When the total amplitude imbalance is K dB, (1) is given by

$$I_{\rm leak} = \sqrt{I'^2_{\rm A} + \left(10^{-\frac{K}{20}} \cdot I'_{\rm A}\right)^2 - 2 \cdot I'_{\rm A} \cdot 10^{-\frac{K}{20}} \cdot I'_{\rm A} \cdot \cos\theta} \tag{2}$$

where

$$K = \left| 20 \log \frac{I'_{\rm B}}{I'_{\rm A}} \right|.$$

The LO suppression ratio $S_{\rm LO}$ is defined as the ratio of $I_{\rm leak}$ to LO input current $I_{\rm IN}$. Therefore, $S_{\rm LO}$ is given by

$$S_{\rm LO}(dB) = -20 \log \frac{I_{\rm leak}}{I_{\rm IN}}. \tag{3}$$

Given that LO input current $I_{\rm A} + I_{\rm B}$ is equal to $\sqrt{2} I'_{\rm A}$, from (3) we can obtain

$$\begin{aligned} S_{\rm LO}(dB) &= -20 \log \frac{\sqrt{I'^2_{\rm A} + \left(10^{-\frac{K}{20}} \cdot I'_{\rm A}\right)^2 - 2 \cdot I'_{\rm A} \cdot 10^{-\frac{K}{20}} \cdot I'_{\rm A} \cdot \cos\theta}}{\sqrt{2} I'_{\rm A}} \\ &= -10 \log \frac{1 + 10^{-\frac{K}{10}} - 2 \cdot 10^{-\frac{K}{20}} \cdot \cos\theta}{2}. \end{aligned} \tag{4}$$

The behavior of LO suppression ratio versus amplitude and phase imbalance is shown in Fig. 2. Assuming that the performance of the unit mixers on an MMIC chip is equal, amplitude and phase imbalance is dominated by the quadrature couplers. For example, when $K = 0$ dB, in order to achieve an LO suppression ratio over 40 dB, a phase imbalance of less than 0.8° is required within a particular frequency range.

III. MMIC Dual-Quadrature Up-Converter Elements

A. Multilayer Directional Coupler

Our up-converter employs multilayer directional couplers [3] with a multilayer MMIC technique for high-performance 3-dB quadrature couplers. A cross-sectional view of the multilayer directional coupler is shown in Fig. 3. This coupler is applied as the divider/combiner circuit of the dual-quadrature up-converter shown in Fig. 1. The multilayer structure consists of four 2.5-μm-thick polyimide films ($\epsilon_{\rm r} = 3.7$) for dielectric layers fabricated on a GaAs substrate and 1-μm-thick gold

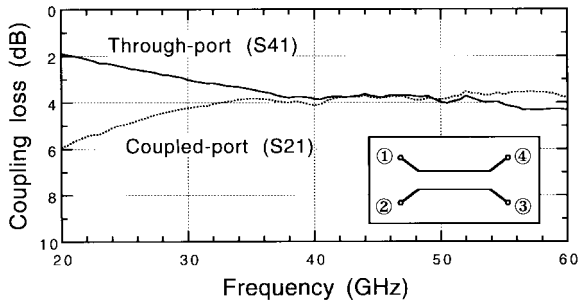

(a)

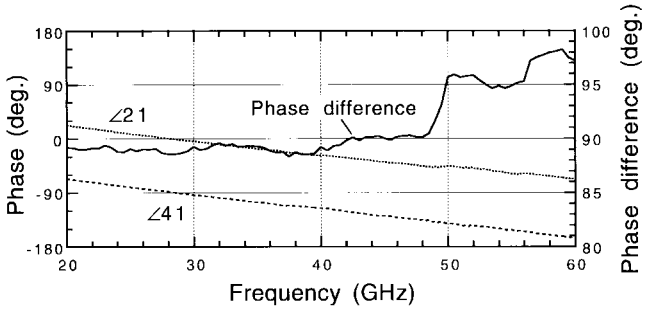

(b)

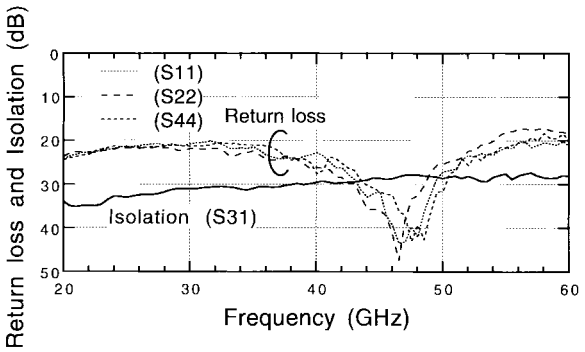

(c)

Fig. 4. Measured performance of the multilayer directional coupler: (a) coupling loss; (b) phase and phase differential; and (c) return loss and isolation.

films for the conductor metals. The thickness of the GaAs substrate is 450 μm. The directional coupler is constructed with coupled microstrip lines, a ground conductor with a tuning septum, and a floating conductor located over the coupled microstrip lines. The coupled microstrip lines are 720 μm in length. Each conductor is formed on its own dielectric layer of polyimide film. This structure makes it possible to realize the high even-mode to odd-mode impedance ratio required to achieve coupling on the order of 3 dB. By adding a floating conductor, the odd-mode impedance of the microstrip lines can be decreased; by using a septum structure, the even-mode impedance of the microstrip lines can be increased.

The measured performance of the directional coupler used in the dual-quadrature up-converter is shown in Fig. 4. The coupling loss from port 1 to ports 2 and 4 was 3.7 dB, and the phase difference between output ports 2 and 4 was $90^\circ \pm 0.2^\circ$ from 42 to 48 GHz. Isolation was greater than 28 dB, and return losses were greater than 23 dB from 42 to 48 GHz. As the figure shows, since this directional coupler has

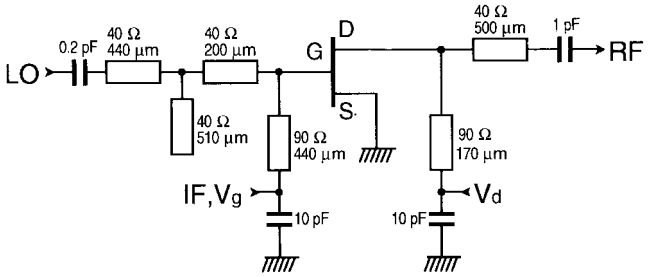

Fig. 5. Equivalent circuit of the unit mixer used for the up-converter.

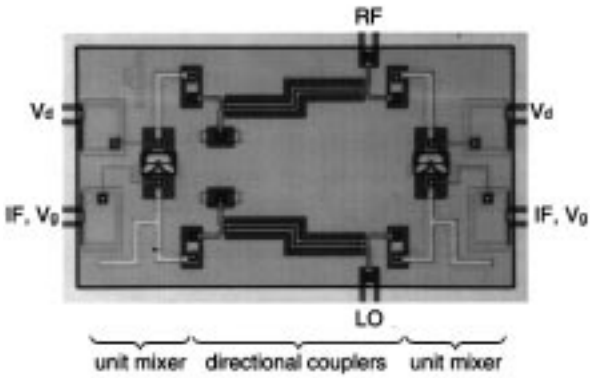

Fig. 6. A photograph of the fabricated MMIC dual-quadrature up-converter.

perfect amplitude balance, a low-coupling loss, and accurate quadrature phase difference, it is well suited for use in the dual-quadrature up-converter.

B. Unit Mixer

The equivalent circuit of the unit mixers is shown in Fig. 5. As shown in this figure, a gate mixer configuration [6] is employed in the unit mixers; the intermediate frequency (IF) and local oscillator (LO) signals are applied to the field-effect transistor (FET) gate and the RF signal is taken from the drain. The impedance matching networks consist of thin-film microstrip lines [5] and metal–insulator–metal (MIM) capacitors, which block a dc. The IF input signal and the gate voltage are fed through an open stub for LO port impedance matching. The active device uses a heterojunction FET [7] with a 100-μm gate width and a 0.2-μm gate length. The device has an $F_{\rm t}$ and $F_{\rm max}$ of 80 and 130 GHz, respectively.

IV. Performance of the MMIC Dual-Quadrature Up-Converter

A photograph of the fabricated MMIC dual-quadrature up-converter is shown in Fig. 6. The up-converter elements described above are integrated on a single chip, whose size is 1.28 mm $\times$ 2.34 mm.

On-wafer probes were used to evaluate the performance of the MMIC up-converter. Using a commercially available IF 180° hybrid, the performance of the up-converter was measured with a 6-dBm LO input. The IF frequency was set at 1 GHz. The FET drain bias was 3 V, and the drain current was 20 mA.

The measured RF output power and simulated and measured LO leakage of the up-converter as a function of LO frequency

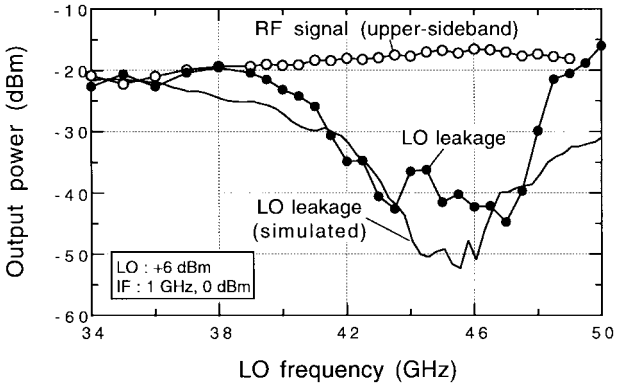

Fig. 7. Measured RF output power and simulated and measured LO leakage of the up-converter as a function of LO frequency.

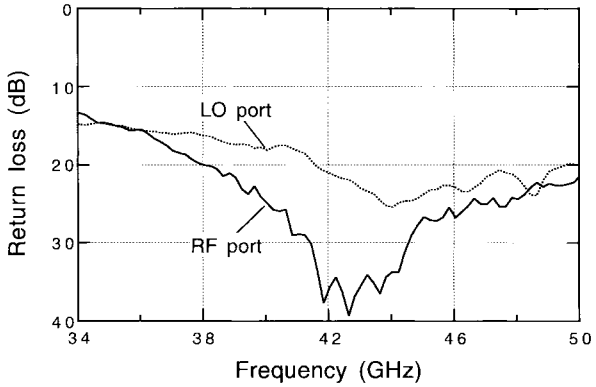

Fig. 8. Measured return loss at RF and LO ports of the up-converter.

are shown in Fig. 7. LO leakage was linearly simulated with Libra (HP-EEsof Inc.) using ideal coupler and unit mixer performance. For upper-sideband frequencies, conversion loss was less than 17 ± 1 dB for LO frequencies from 42.5–47.5 GHz. LO leakage power suppression was 22 ± 4 dB lower than the up-converted upper-sideband signal, and it was confirmed that the simulated LO leakage value agreed with the measured value. The up-converter achieved an LO leakage suppression of over 40 dB compared to LO input power (+6 dBm). The high LO leakage suppression was achieved by the good amplitude balance and accurate 90° phase difference of the multilayer directional couplers. Since the two unit mixers were considered to have identical performance, this LO leakage suppression agreed well with the values obtained from (4) and in Fig. 2. On the other hand, the measured IF to RF port isolation was over 30 dB. In the up-converter, filtering the IF leakage signal at the RF port is easy because the IF frequency is low and very far from the RF frequency.

The measured return losses at the RF and LO ports are shown in Fig. 8. RF return loss is greater than 20 dB over 38 GHz, and LO return loss is also greater than 20 dB over 41 GHz. As shown in this figure, the dual-quadrature up-converter has good RF and LO return loss.

Fig. 9 shows the measured RF output power of upper-sideband frequencies as a function of IF input power at an LO frequency of 47.5 GHz. The up-converter has an output 1-dB compression point of -7.5 dBm and a saturated RF output power of -5 dBm for upper-sideband frequencies.

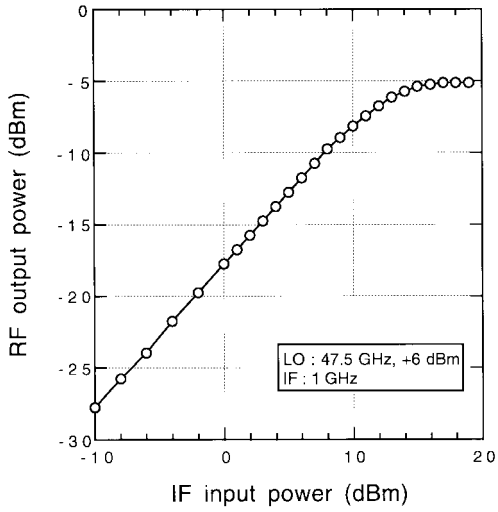

Fig. 9. Measured upper-sideband output power of the up-converter.

V. Conclusion

A millimeter-wave band MMIC dual-quadrature up-converter with good LO suppression has been developed. The up-converter consists of two unit mixers and two high-performance multilayer directional couplers. These high-performance directional couplers enable large LO suppression. In an LO frequency range from 42.5 to 47.5 GHz, the MMIC up-converter achieved a conversion loss of less than 17 ± 1 dB, and LO was suppressed 22 ± 4 dB lower than the desired RF output signal, which is the greatest value among those reported. The developed up-converter will be applied to millimeter-wave communication systems in the near future.

Acknowledgment

The authors would like to thank Dr. K. Habara, Dr. H. Inomota, and Dr. E. Ogawa for their continuous support and encouragement. They also wish to thank Dr. Y. Harada, M. Sawada, and K. Nagami of SANYO Electric Co., Ltd. for their help in fabricating the MMIC's.

References

[1] T. Hirota and H. Okazaki, "Compact and wideband MMIC frequency converters," in *25th Eur. Microwave Conf. Proc.*, Sept. 1995, pp. 1097–1100.

[2] H. Wang, B. Nelson, L. Shaw, R. Kasody, Y. Hwang, W. Jones, D. Brunone, M. Sholly, J. Maguire, and T. Best, "A monolithic V-band upconverter using 0.2 μm InGaAs/GaAs pseudomorphic HEMT technology," in *IEEE MTT-S Int. Microwave Symp. Dig.*, June 1992, pp. 1059–1062.

[3] S. Banba and H. Ogawa, "Multilayer MMIC directional couplers using thin dielectric layers," *IEEE Trans. Microwave Theory Tech.*, vol. 43, no. 6, pp. 1270–1275, June 1995.

[4] T. Hiraoka, T. Tokumitsu, and M. Aikawa, "Very small wide-band MMIC magic-T's using microstrip lines on a thin dielectric film," *IEEE Trans. Microwave Theory Tech.*, vol. 37, pp. 1569–1575, Oct. 1989.

[5] T. Tokumitsu, T. Hiraoka, H. Nakamito, and T. Takenaka, "Multilayer MMIC using a 3 μm $\times$ 3-layer dielectric film structure," in *IEEE MTT-S Int. Microwave Symp. Dig.*, May 1990, pp. 831–834.

[6] C. C. Peñalosa and C. Aitchison, "Analysis and design of MESFET gate mixer," *IEEE Trans. Microwave Theory Tech.*, vol. MTT-35, pp. 643–652, July 1987.

[7] M. Sawada, D. Inoue, K. Matsumura, and Y. Harada, "A new two-mode channel FET (TMT) for super-low-noise and high-power applications," *IEEE Electron Device Lett.*, vol. 14, pp. 354–356, July 1993.

Akira Minakawa (M'96) received the B.S. and M.S. degrees in electrical engineering from Ibaraki University, Ibaraki, Japan, in 1984 and 1986, respectively.

He joined the NTT Radio Communication Networks Laboratories, Yokosuka, Japan, in 1986. He has been engaged in research and development of MMIC's. From 1993 to 1995, he worked in research on millimeter-wave integrated circuits for personal communication systems at ATR Optical and Radio Communications Research Laboratories. Since 1996, he has been researching MMIC's for communication satellites at NTT Wireless Systems Laboratories, Yokosuka, Japan.

Mr. Minakawa is a member of the Institute of Electronics, Information and Communication Engineers (IEICE) of Japan.

Toshikazu Imaoka (M'96) received the B.E. degree in electrical engineering from Osaka Prefecture University, Osaka, Japan, in 1984.

In 1984, he joined the Microelectronics Research Center of SANYO Electric Company, Ltd., Osaka, Japan, where he did research and development work on microwave devices. From 1994 to 1996, he worked in research on millimeter-wave integrated circuits for personal communication systems at ATR Optical and Radio Communications Research Laboratories. He is now with ATR Adaptive Communications Research Laboratories, Kyoto, Japan.

Mr. Imaoka is a member of the Institute of Electronics, Information and Communication Engineers (IEICE) of Japan.

Nobuaki Imai (M'96) received the B.S. degree in electrical engineering from Nagoya Institute of Technology, Nagoya, Japan, in 1975, and the M.S. degree from Kyoto University, Kyoto, Japan, in 1977.

He joined Yokosuka Electrical Communications Laboratories, Japan, in 1977, where he was engaged in research on microwave and millimeter-wave integrated circuits and the development of digital microwave radio systems. In 1993, he moved to ATR Optical and Radio Communications Research Laboratories, where he has been engaged in research of millimeter-wave personal communication systems using optical fiber. He is now with ATR Adaptive Communications Research Laboratories, Kyoto, Japan.

Mr. Imai is a member of the Institute of Electronics, Information and Communication Engineers (IEICE) of Japan.